

# A Virtual Screening Approach For Identifying Plants with Anti H5N1 Neuraminidase Activity

Nur Kusaira Khairul Ikram,<sup>†,‡</sup> Jacob D. Durrant,<sup>§</sup> Muchtaridi Muchtaridi,<sup>‡,||</sup> Ayunni Salihah Zalaludin,<sup>†</sup> Neny Purwitasari,<sup>||</sup> Normisah Mohamed,<sup>||</sup> Aisyah Saad Abdul Rahim,<sup>||</sup> Chan Kit Lam,<sup>||</sup> Yahaya M. Normi,<sup>⊥</sup> Noorsaadah Abd Rahman,<sup>#</sup> Rommie E. Amaro,<sup>§</sup> and Habibah A Wahab<sup>\*,†,‡,||</sup>

<sup>†</sup>Malaysian Institute of Pharmaceuticals and Nutraceuticals, Ministry of Science, Technology and Innovation, Jalan Bukit Gambir, 11800, Penang, Malaysia

<sup>‡</sup>Pharmaceutical Design and Simulation Laboratory (PhDs), School of Pharmaceutical Sciences, Universiti Sains Malaysia, 11800, Penang, Malaysia

<sup>§</sup>Department of Chemistry & Biochemistry and the National Biomedical Computation Resource, University of California—San Diego, La Jolla, California 92093-0340, United States

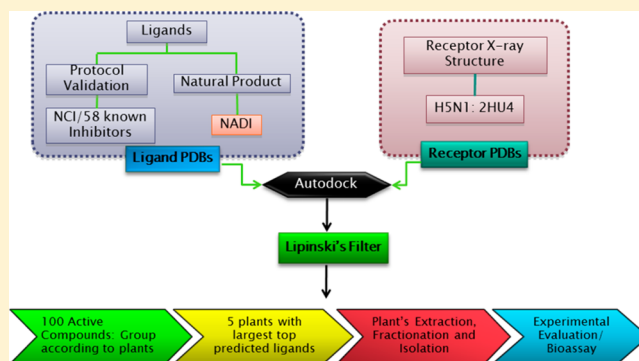
<sup>||</sup>School of Pharmaceutical Sciences, Universiti Sains Malaysia, 11800, Penang, Malaysia

<sup>⊥</sup>Department of Cell and Molecular Biology, Faculty of Biotechnology and Biomolecular Sciences, Universiti Putra Malaysia, 43400 Serdang, Selangor, Malaysia

<sup>#</sup>Department of Chemistry, Universiti Malaya, 50603, Kuala Lumpur, Malaysia

## Supporting Information

**ABSTRACT:** Recent outbreaks of highly pathogenic and occasional drug-resistant influenza strains have highlighted the need to develop novel anti-influenza therapeutics. Here, we report computational and experimental efforts to identify influenza neuraminidase inhibitors from among the 3000 natural compounds in the Malaysian-Plants Natural-Product (NADI) database. These 3000 compounds were first docked into the neuraminidase active site. The five plants with the largest number of top predicted ligands were selected for experimental evaluation. Twelve specific compounds isolated from these five plants were shown to inhibit neuraminidase, including two compounds with IC<sub>50</sub> values less than 92 μM. Furthermore, four of the 12 isolated compounds had also been identified in the top 100 compounds from the virtual screen. Together, these results suggest an effective new approach for identifying bioactive plant species that will further the identification of new pharmacologically active compounds from diverse natural-product resources.



## INTRODUCTION

Influenza remains a serious health threat and a future pandemic risk, as evidenced by recent outbreaks of H5N1 and H1N1.<sup>1–3</sup> These influenza type A strains, which cause acute upper respiratory tract infections<sup>1</sup> with high morbidity and mortality, possess three viral-coat proteins: hemagglutinin (HA), neuraminidase (NA), and M2. HA and NA are glycoproteins that recognize terminal sialic-acid (SA) residues on host-cell surface receptors, and M2 is a proton channel critical for virus assembly and replication.<sup>4</sup> Upon attachment via SA binding, HA mediates viral entry into the cell. Following viral replication, NA facilitates the liberation of new virions from the cellular surface by cleaving the α(2–6)- or α(2–3)-ketosidic linkages that connect terminal SA residues to cell-surface glycoproteins.<sup>5–7</sup> NA is conserved in all wild-type influenza viruses, and its inhibition halts viral propagation by interfering with effective shedding. Consequently, it is an attractive target for anti-influenza drug design.<sup>8</sup>

WHO recommends stockpiling NA inhibitors<sup>9</sup> such as zanamivir (Relenza, GlaxoSmithKline) and oseltamivir (Tamiflu, Roche),<sup>10,11</sup> which have recently replaced older drugs like rimantadine and amantadine.<sup>9,12</sup> However, the threat of an H1N1 flu pandemic,<sup>13</sup> the sudden emergence of oseltamivir-resistant H1N1,<sup>14</sup> and the emergence of potentially pathogenic H3N2<sup>15</sup> and H5N1<sup>16</sup> strains warrant ongoing efforts to identify novel anti-influenza compounds. Consequently, many researchers have expended considerable effort in the pursuit of antiviral small molecules via bioinformatics studies, hit-and-lead discovery approaches, and analogue synthesis.<sup>17–23</sup>

Natural compounds constitute an indispensable source of potential inhibitors from which these studies can draw.<sup>24,25</sup>

Received: July 8, 2014

Published: January 2, 2015

For example, the plant flavonoids isoscutellarein and isoscutellarein-8-methyl ether, derived from the leaves and roots of *Scutellaria baicalensis*, have been known to inhibit H1N1 NA since 1995.<sup>26</sup> In total, about 160 similar plant compounds have been isolated and tested to date (reviewed in ref 27).

Inspired by the wealth and diversity of Malaysian tropical plants, we recently developed the Natural Product Discovery (NADI) repository (<http://www.nadi-discovery.com/>)<sup>28</sup> as an online resource. This resource consists of several databases, including NADI-MEPS, which describes the ethnopharmacological use of various Malaysian plants, and NADI-CHEM, which stores the three-dimensional structures of over 3000 compounds from more than 250 Malaysian plants for use in computational-biology studies.

Virtual screening has shown great promise in sorting through large libraries of potential bioactive molecules like those in the NADI repository.<sup>29–32</sup> For example, in 2008, Rollinger et al. demonstrated how natural-product/ethnopharmacological-guided virtual screening can be used to select a particular class of natural products for subsequent study. Compounds they isolated from the gum resin asafetida yielded four experimentally confirmed inhibitors that were subsequently shown to inhibit human rhinovirus in the low micromolar range. Two of these compounds were present among their original virtual hits.<sup>33</sup>

Here, we report a similar virtual screen of the NADI compound database aimed at influenza drug discovery. Although the NADI provides useful ethnopharmacological information about each plant, we aimed to blindly predict the activity of each compound *in silico* without regard for traditional regional medical practices. The top predicted inhibitors principally came from five distinct plants: *Garcinia mangostana*, *Eurycoma longifolia*, *Tabernaemontana divaricata*, *Brucea javanica*, and *Momordica charantia*. These plants were subjected to *in vitro* evaluation in order to characterize H5N1 NA inhibition. All the plant extracts demonstrated some inhibitory activity; *G. mangostana* extracts yielded the highest percent inhibition (82.95% at 250  $\mu\text{g}/\text{mL}$ ).

Fractions obtained from the extracts of these plants were subsequently tested for NA activity, ultimately leading to the isolation of 12 compounds from *G. mangostana* (4), *M. charantia* (2), *B. javanica* (1), *T. divaricata* (1), and *E. longifolia* (4) that also inhibited H5N1 neuraminidase. Of these 12 compounds, four had already been identified as hits in our initial NADI virtual screen.

We are hopeful that the virtual-screening methodology described here will become an increasingly effective tool for rapidly identifying bioactive plants for additional experimental study.

## METHODS

**Molecular Docking.** The three-dimensional structures of ~3000 NADI and ~2000 NCI compounds were obtained from [www.nadi-discovery.com](http://www.nadi-discovery.com) and [dtp.nci.nih.gov](http://dtp.nci.nih.gov), respectively. Compounds that did not satisfy Lipinski's rule of five for drug-likeness were discarded.<sup>34</sup> An additional 58 known inhibitors of Neuraminidase A with  $K_i$  or  $\text{IC}_{50}$  values less than or equal to 25 nM were identified using the BindingDB database.<sup>35,36</sup> Structures of these compounds were generated using Schrödinger's LigPrep module (2011). In brief, protonation states were assigned at pH 7.0 using Epik.<sup>37,38</sup> For each compound, LigPrep identified all tautomeric and one stereoisomeric state. Where appropriate, one low-energy ring conformation was determined per ligand. The geometry of the known inhibitors was optimized using the OPLS\_2005 force field.<sup>39,40</sup>

Both the small molecules and the H5N1 NA receptor were prepared for docking using the AutoDockTools (ADT) software package.<sup>41</sup> The receptor was prepared from an X-ray crystal structure of H5N1 neuraminidase (PDB ID: 2HU4).<sup>42</sup> Hydrogen atoms were added to all ligands and NA models using ADT, and ligand rotatable bonds were assigned via AutoTors.<sup>43</sup> Default Kollman charges<sup>44</sup> and solvation parameters were assigned to the protein atoms. Gasteiger charges were added to each ligand atom.<sup>45</sup> Grid boxes comprised of  $60 \times 60 \times 60$  points spaced 0.375 Å apart and centered on the NA active site were calculated for the following atom types: C, A (aromatic C), N, O, S, H, F, Cl, Br, I, P, and e (electrostatic) using Autogrid3.<sup>43</sup>

AutoDock 3.0.5<sup>43,46</sup> was used for the docking simulation. The parameters of the Lamarckian Genetic Algorithm (LGA) were as follows: population size of 50, elitism of 1, mutation rate of 0.02, crossover rate of 0.80, local search rate of 0.06, 250 000 energy evaluations, and 100 search runs. The final docked conformations were clustered using a cluster tolerance of 1.0 Å root-mean-square deviation (RMSD). The ligand pose with the lowest predicted free energy of binding, chosen from the most populated cluster, was used in subsequent analysis.

**Natural Product Isolation.** *Chemicals and Reagents.* Solvents used for extraction and column chromatographic analysis were of analytical grade (AR), and solvents used in the liquid chromatographic analysis were of HPLC grade. Reagents and solvents were purchased from the Central Store, Universiti Sains Malaysia. H5N1 neuraminidase was obtained from SINOBIO (China). MUNANA [2'-2-(4-methylumbelliferyl)-a-D-N-acetylneuraminic acid sodium salt hydrate], MES [2-(*N*-morpholino)ethanesulfonic acid], and DANA [2,3-didehydro-2-deoxy-N-acetylneuraminic acid] were obtained from SIGMA (Malaysia).

*Instruments.* Melting points were determined using a SMP20 melting point apparatus (Stuart) and a differential scanning calorimeter (PerkinElmer). FTIR spectra were recorded using an IR Prestige-21 instrument (Shimadzu) and a Nicolet 6700 FTIR-ATR spectrometer (Thermo Scientific) available at the Centre for Drug Research, Universiti Sains Malaysia. UV spectra were recorded using a U-2000 spectrophotometer (Hitachi, Japan) and a UV 1601PC spectrophotometer (Shimadzu). MS spectra were acquired using a 1100 series LC-MSD Trap G2445L (Agilent Technologies, Palo Alto, USA).

<sup>1</sup>H and <sup>13</sup>C NMR spectra were both recorded at 500 MHz using an AVANCE III HD Spectrometer (Bruker). Semipolar compounds were dissolved in deuterated chloroform ( $\text{CDCl}_3$ ), and polar compounds were dissolved in 99%  $\text{CD}_3\text{OD}$ . A centrifugal TLC (Cyclograph, Analtech Inc.; Newark, DE, USA) was used to separate fractions. Sample purification was achieved using a PU-980 HPLC system (Jasco; Tokyo, Japan) equipped with a solvent delivery pump, a 772Si sample injector (Rheodyne; Cotati, CA, USA) with a 250  $\mu\text{L}$  sample loop, a UV-975 detector (Jasco; Tokyo, Japan), and a D-2500 Chromato-integrator (Hitachi; Tokyo, Japan). Mass spectra were measured on a 1100 series LC-MSD Trap G2445 VL (Agilent Technologies, Palo Alto, California, USA). The HPLC system was used to check for peak purity. A microplate reader (Turner-Biosystem, USA) was used to measure neuraminidase inhibition.

*Plant Materials.* *G. mangostana* fruits were purchased from Balik Pulau, Penang. The hulls were air-dried and powdered with a mechanical grinder. *M. charantia* was purchased from Bayan Baru, Penang. The leaves were oven-dried (45 °C) and powdered. The leaves of *T. divaricata* were collected around Penang, oven-dried (45 °C), and powdered. The seeds of *B. javanica* were obtained from Solo, East Java, Indonesia, and

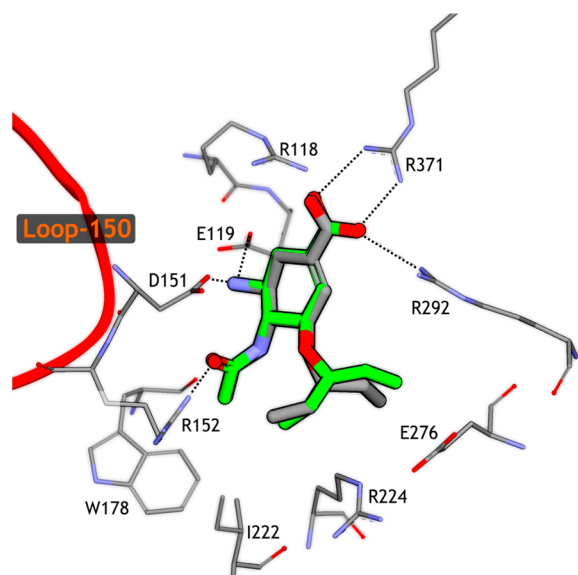


**Figure 1.** Superimposition of the docked and crystallographic oseltamivir poses (green and blue, respectively). The RMSD was 0.84 Å. Note also that the interacting residues are similar for both poses.

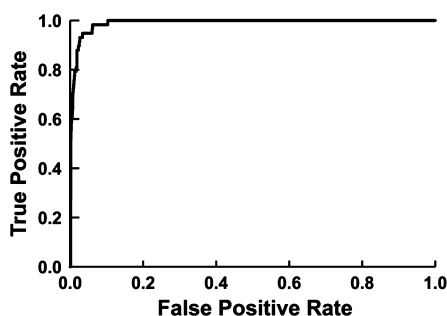


**Figure 2.** Receiver operator curve generated from the initial benchmark screen of the NCI Diversity Set I (presumed decoys) and known potent NA inhibitors. The area under the curve is 0.99, suggesting the screening methodology is highly predictive.

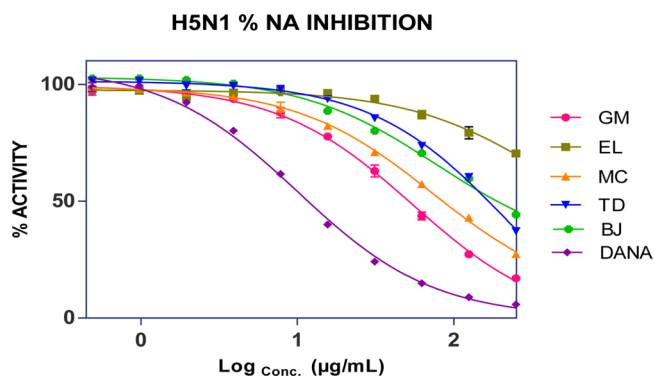


**Figure 3.** Percent H5N1 NA inhibition of five plant MeOH extracts (250–0.488  $\mu\text{g/mL}$ ). The calculated  $\text{IC}_{50}$  for the plant extracts are *G mangostana* =  $50.93 \pm 0.02 \mu\text{g/mL}$ , *M charantia* =  $79.43 \pm 0.06 \mu\text{g/mL}$ , *B. javanica* =  $184.93 \pm 0.04 \mu\text{g/mL}$ , *T. divaricata* =  $164.81 \pm 0.03 \mu\text{g/mL}$ .

were likewise dried and ground into powder. *E. longifolia* plant and root samples were identified and purchased in Perak, Malaysia, by the pharmaceutical company Hovid Berhad (Ipoh). Voucher specimens for all the plant materials with the exception of *E. longifolia* were deposited in the Herbarium of the School of

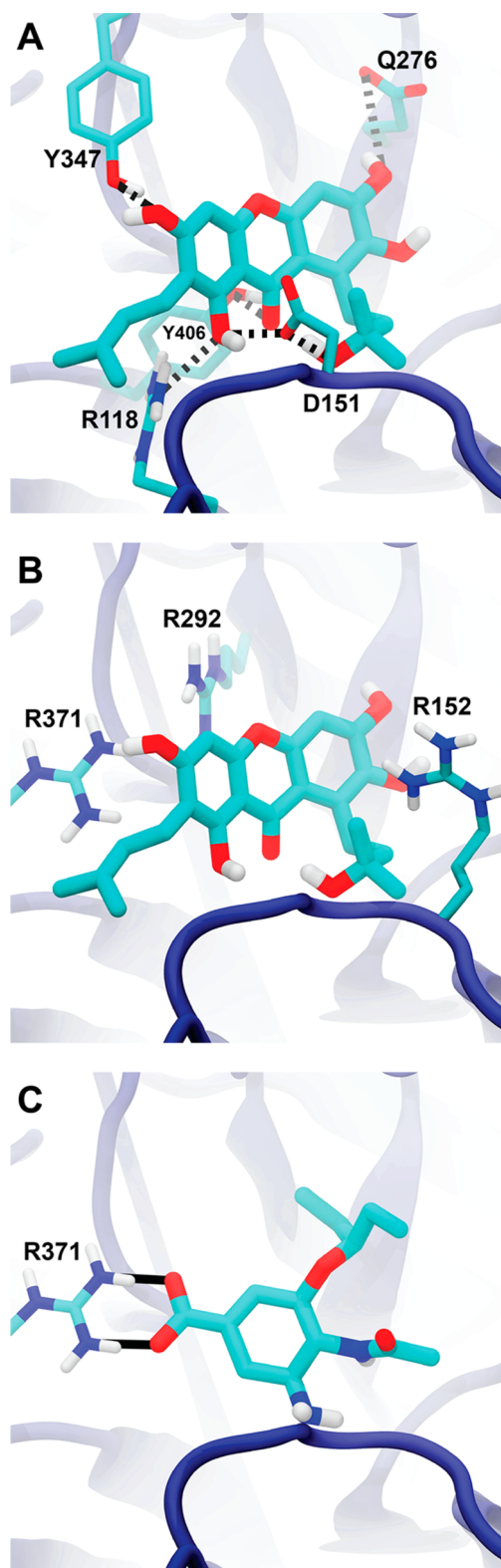


**Figure 4.** Predicted pose of Garcinone C, docked into the neuraminidase active site. (A) Predicted hydrogen bonds. (B) Predicted cation- $\pi$  interactions between R371, R292, R152, and the xanthone moiety. (C) The crystallographic pose of oseltamivir, a potent inhibitor, shown for reference (PDB ID: 2HU4).

Biological Sciences, Universiti Sains Malaysia (No. 11301, 11302, 1298, and 1299 for *G. mangostana*, *M. charantia*, *T. divaricata*, and *B. javanica*, respectively). An *E. longifolia* voucher specimen

Table 1. Percent NA Inhibition of Plant Fractions Selected Based on Virtual Screening

plant	% inhibition of HSN1 NA at 250 $\mu\text{g}/\text{mL}$						
	extract	fraction					
	EXT	F1	F2	F3	F4	F5	F6
<i>G. mangostana</i>	82.95 $\pm$ 0.21	83.73 $\pm$ 0.28	78.25 $\pm$ 0.05	84.49 $\pm$ 0.19	80.15 $\pm$ 0.27		
<i>M. charantia</i>	72.61 $\pm$ 0.34	58.03 $\pm$ 0.39	34.12 $\pm$ 0.10	70.70 $\pm$ 0.47	72.43 $\pm$ 0.13	46.93 $\pm$ 0.17	66.08 $\pm$ 0.20
<i>T. divaricata</i>	62.79 $\pm$ 0.20	35.95 $\pm$ 0.19	20.06 $\pm$ 0.05	33.47 $\pm$ 0.11	28.00 $\pm$ 0.23	20.95 $\pm$ 0.09	11.90 $\pm$ 0.21
<i>B. javanica</i>	55.80 $\pm$ 0.03	49.64 $\pm$ 0.44	58.38 $\pm$ 0.12	57.49 $\pm$ 0.03			
<i>E. longifolia</i>	29.62 $\pm$ 0.36	9.14 $\pm$ 0.22	8.00 $\pm$ 0.36	23.02 $\pm$ 0.30	56.47 $\pm$ 0.17		

(No. 785–117) was deposited in the Penang Botanical Garden, Penang, Malaysia.

A description of the extraction, fractionation, and isolation of specific compounds can be found in the Supporting Information, together with experimentally measured purities, melting points, and IR/NMR spectra.

**Bioassay.** Neuraminidase activity was measured by modifying the method of Potier et al.<sup>47</sup> MUNANA (SIGMA, M8639) in 32.5 mM MES (SIGMA, M8250) buffer (pH 6.5) served as the substrate, and neuraminidase from viral HSN1 (SINO BIO) in MES buffer served as the enzyme. The chemical compounds, plant extracts, and fractions were dissolved in 2.5% DMSO and diluted to various concentrations ranging from 0.488  $\mu\text{g}/\text{mL}$  to 250  $\mu\text{g}/\text{mL}$  in MES buffer. For the assay, neuraminidase (25  $\mu\text{L}$ ) was added to 25  $\mu\text{L}$  of sample solution mixed with a buffer in 96-well microplates. 50  $\mu\text{L}$  of substrate was then added and incubated at 37  $^{\circ}\text{C}$ . After 1 h, 100  $\mu\text{L}$  of stop solution was added to each well, and 4-methylumbelliferone was immediately quantified fluorometrically using a Modulus Microplate Reader (Turner Biosystem, USA). The excitation and emission wavelengths were set at 365 and 450 nm, respectively. Assay measurements were carried out in triplicate. The percentage of NA inhibition over a range of compound concentrations was determined by fitting experimental data to the logistic graph. DANA and oseltamivir carboxylate were used as standard inhibitors (positive controls) in the bioassay. The detergent assay was adapted from the work of Feng and Shoichet,<sup>48</sup> by adding 0.01% Triton-X-100 to the MES buffer.

## RESULTS

**Validation of the Virtual-Screening Protocol.** Prior to performing a virtual screen of the NADI database using AutoDock 3.05,<sup>46</sup> we first validated our docking procedure. An oseltamivir molecule was extracted from a crystallographic NA structure (PDB ID: 2HU4<sup>42</sup>) and redocked into the same binding pocket. The docked ligand pose was similar to the crystallographic pose (RMSD = 0.84  $\text{\AA}$ , Figure 1), demonstrating that the AutoDock docking parameters used are amenable to this system.

We next verified that our virtual-screening technique was capable of identifying known NA inhibitors. The compounds of the NCI Diversity Set 1 (presumed decoys/negatives), together with 58 known neuraminidase A inhibitors with  $K_i$  or  $\text{IC}_{50}$  values less than or equal to 25 nM (positives), were docked using the same protocol described above. The area under the ROC curve generated from this initial benchmark screen was 0.99 per the trapezoidal rule (Figure 2), suggesting that our screening methodology is highly predictive.

**Screening the NADI Database.** Satisfied that our virtual-screening protocol could be effectively used to identify NA inhibitors, we next performed a virtual screen of  $\sim$ 3000 NADI

compounds. The top 100 compounds with the best docking scores (Table S1) were derived from a total of 31 local Malaysian plants. *G. mangostana*, *E. longifolia*, *T. divaricata*, *M. charantia*, and *B. javanica* possessed the greatest number of predicted HSN1 inhibitors (Table S2) and so were selected for further experimental evaluation.

Methanol (MeOH) extracts of these five plants (Figure 3), as well as their fractions (Table 1 and Figure S1), were tested for HSN1 NA inhibition. With the exception of *E. longifolia*, all plants showed marked NA inhibition. *G. mangostana*, *M. charantia*, *T. divaricata*, *B. javanica*, and *E. longifolia* had 82.95%, 72.61%, 62.79%, 55.80%, and 29.62% NA inhibition at 250  $\mu\text{g}/\text{mL}$ , respectively. In general, isolated fractions of these plant extracts (Table 1) also inhibited neuraminidase. Fraction F3 from *G. mangostana* had 84.49% inhibition, fractions F3 and F4 from *M. charantia* had >70% inhibition, all three *B. javanica* fractions had >50% inhibition, and *T. divaricata* had only modest inhibition (12 to 36%). Interestingly, though the inhibition of the whole MeOH *E. longifolia* extract was negligible, fraction F4 from this species did demonstrate reasonable inhibition (56.47%).

Efforts were next undertaken to isolate specific inhibitory compounds from the extracts of these five plants. Within the time frame of the experiment, we isolated 12 compounds from the fractions of *G. mangostana* (4), *M. charantia* (2), *T. divaricata* (1), *B. javanica* (1), and *E. longifolia* (4) (Table 2 and Figure S2). Of these 12 compounds, five compounds showed >50% inhibition at 250  $\mu\text{g}/\text{mL}$ , with  $\text{IC}_{50}$  values ranging from 89.71 to 275.45  $\mu\text{M}$ . Four of the 12 compounds were present in the original virtual screen, including gartanin, with an  $\text{IC}_{50}$  value of 126.64  $\pm$  0.13  $\mu\text{M}$  (Table 2). An additional four compounds (rubraxanthone, kuguacin J, 13 $\alpha$ ,21-dihydroeurycomanone, and 13 $\alpha$ ,21-epoxyeurycomanone) were absent from the NADI database at the time of screening and so could not have been identified *in silico*. In contrast,  $\alpha$ -mangostin, garcinone C, eurycomanol, and daucosterol failed to rank among the top 100 hits of the virtual screen (Table S1).

Momordicin I and kuguacin J from *M. charantia* showed 15.58% and 21.42% NA inhibition, respectively. Voaphylline from *T. divaricata* showed 20.95% inhibition. Daucosterol from *B. javanica* showed 60.65% inhibition ( $\text{IC}_{50}$  of 275.45  $\pm$  0.03  $\mu\text{M}$ ), far better than any of the fractions or extracts from this species. As expected, the compounds from *E. longifolia* exhibited low inhibition, never exceeding the 34.50% inhibition of 13 $\alpha$ , 21-epoxyeurycomanone.

All four compounds from *G. mangostana* demonstrated >80% inhibition at 250  $\mu\text{g}/\text{mL}$ , with  $\text{IC}_{50}$  values of 91.95  $\pm$  0.09, 89.71  $\pm$  0.08, 95.49  $\pm$  0.08, and 126.64  $\pm$  0.13  $\mu\text{M}$  for  $\alpha$ -mangostin, rubraxanthone, garcinone C, and gartanin, respectively.  $\alpha$ -Mangostin and gartanin have been previously isolated from *G. mangostana* pericarps and have been shown to inhibit *C. perfringens* neuraminidase with  $\text{IC}_{50}$  values of 12.2  $\pm$  1.2 and 2.9  $\pm$  0.3  $\mu\text{M}$ , respectively.<sup>49</sup> The presence of  $\alpha$ -mangostin, gartanin, and

Table 2. AutoDock Score, IC<sub>50</sub> Values, and Percent Inhibition of Compounds Isolated from Five Plants<sup>a</sup>

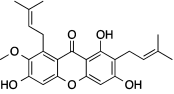
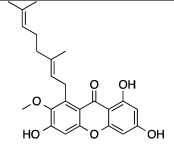
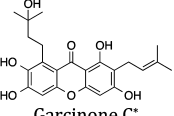
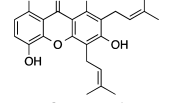
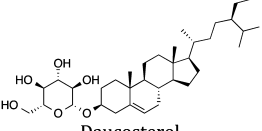
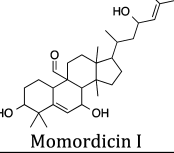
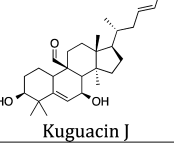
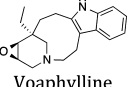
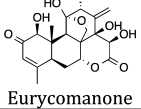
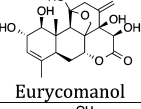
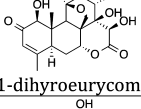
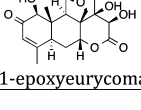
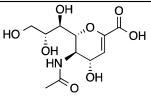
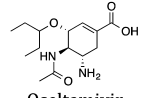
Compounds	AutoDock score (kcal/mol)	IC <sub>50</sub> (μM)	% inhibition (at 250 μg/ml)
 α-mangostin*	-8.87	91.95±0.09	93.08±0.04 (at 609 μM)
 Rubraxanthone*	-9.85	89.71±0.08	92.42±0.12 (at 609 μM)
 Garcinone C*	-8.85	95.49±0.08	90.13±0.02 (at 603 μM)
 Gartanin*	-11.07	126.64±0.13	80.25±0.32 (at 631 μM)
 Daucosterol	-8.99	275.45±0.03	60.65±0.29 (at 433 μM)
 Momordicin I	-11.49	≥250	15.58±0.36 (at 529 μM)
 Kuguacin J	-10.21	≥250	21.42±0.50 (at 550 μM)
 Voaphylline	-10.49	≥250	20.95±0.09 (at 800 μM)
 Eurycomanone	-10.89	≥250	20.84±0.67 (at 612 μM)
 Eurycomanol	-9.83	≥250	21±0.18 (at 609 μM)
 13α,21-dihydroeurycomanone	-9.92	≥250	2.90±0.34 (at 631 μM)
 13α,21-epoxyeurycomanone	-10.45	≥250	34.50±0.27 (at 589 μM)

Table 2. continued

Compounds	AutoDock score (kcal/mol)	IC <sub>50</sub> (μM)	% inhibition (at 250 μg/ml)
 DANA		34.82±0.05	94.19±0.02 (at 858 μM)
 Oseltamivir		4.80 E-03	100 (at 879 μM)

<sup>a</sup>Compounds marked with asterisks were subjected to additional testing to rule out nonspecific inhibition by self aggregation.

garcinone C in Asian mangosteen pericarps has been well documented,<sup>50,51</sup> and Lian and Rahmani communicated the presence of rubraxanthone in the Malaysian mangosteen at a recent conference.<sup>52</sup> To our knowledge, however, rubraxanthone has not been previously identified as a neuraminidase inhibitor. These four compounds belong to the xanthones family. It is interesting to note that a series of xanthone derivatives from *C. tricuspidata* has also been shown to inhibit bacterial neuraminidase at the nanomolar level.<sup>53</sup>

Among the 12 NADI compounds tested, compounds from *G. mangostana* showed the highest inhibition rates and were therefore selected for additional testing to rule out inhibition by nonspecific aggregation. According to Feng and Shoichet,<sup>48</sup> most aggregators show a greater than 50% decrease in inhibition in the presence of detergent. The tested compounds demonstrated a 10–15% decrease at 250 μg/mL, far less than 50%. Furthermore, the dose response curve of self-aggregating compounds is typically markedly less steep in the presence of detergent.<sup>54</sup> In contrast, the steepness of the dose response curves of our compounds was unaffected by detergent (Figure S3).

**The Predicted Binding Pose of Garcinone C.** Garcinone C is representative of these xanthone analogues and had a consistent binding pose when docked using two distinct programs (AutoDock 3.05 and Schrödinger's Glide/2011,<sup>55,56</sup> data not shown). We therefore focused on this compound in order to better understand the potential binding modes of these analogues. The AutoDock pose of Garcinone C is shown in Figure 4A and B. Potential interactions between the docked compound and the NA receptor were identified using BINANA,<sup>57</sup> PoseView,<sup>58,59</sup> Visual Molecular Dynamics,<sup>60</sup> and visual inspection. Garcinone C may form hydrogen bonds with the Y347, R118, Y406, D151, and Q276 side chains (Figure 4A), as well as extensive cation- $\pi$  interactions with R371, R292, and R152 (Figure 4B). The crystallographic pose of oseltamivir, a potent approved drug, is shown for reference (Figure 4C).

The predicted binding pose suggests a number of possible optimization routes. For example, the oseltamivir acetamide carbonyl oxygen atom forms a hydrogen bond with the R152 side chain. If the docked pose of Garcinone C is correct, a 2-methylbutan-2-ol moiety is positioned at the same location; the corresponding  $\alpha$ -mangostin and rubraxanthone moieties are entirely hydrophobic. The careful addition of a hydrogen-bond acceptor at this location may improve potency.

Furthermore, all approved neuraminidase inhibitors take advantage of strong electrostatic interactions between negatively charged ligand carboxylate groups and positively charged NA arginine residues, most notably R371. The novel xanthone inhibitors are also predicted to form interactions with active-site arginine side chains via cation- $\pi$  interactions. While these

interactions are substantial, adding negatively charged moieties to the xanthones at the appropriate locations might lead to even stronger electrostatic interactions.

Finally, we note that, like other NA inhibitors, the xanthone compounds are not predicted to bind in the 150-loop cavity.<sup>61,62</sup> Their predicted binding poses are adjacent, however, and moieties could potentially be added to the xanthone scaffold that extend into this highly flexible subpocket.

## DISCUSSION

**Natural Products.** A number of recent medicinal-chemistry studies have applied virtual screening to natural-product databases. For example, a recent virtual screen of 57 natural plant metabolites identified hesperidin and narirutin (isolated constituents of *Citrus junos*), as well as proanthocyanidin, ursolic acid, sitosterol, tangeretin, abbsinone, nobiletin, and tannic acid, as potential H1N1 neuraminidase inhibitors.<sup>63</sup> This work was not validated by bioassay, but hesperidin is known to inhibit influenza growth.<sup>64,65</sup>

Encouraged by this previous success, we aimed to demonstrate that virtual screening can be used to select specific plants from among the rich biodiversity of South East Asia for further *in vitro* pharmacological studies. Despite time and resource restraints, virtual screening proved effective at identifying active botanical/NADI compounds, even when larger-scale efforts were impossible.

**Virtual and Experimental Screening.** To demonstrate that our virtual-screening protocol could effectively identify NA inhibitors, we first docked known NA inhibitors and presumed decoys from the NCI Diversity Set 1. A ROC-curve assessment suggested that our computational protocol was highly predictive.

Given the promising results of our initial NCI benchmark virtual screen, we next applied the same docking protocol to the compounds of the natural product database (NADI). The docking results prompted us to experimentally test five tropical plants for NA inhibition, as described in the Results section. Remarkably, none of these five plants were mentioned in a recent review of 3000 references describing natural-product influenza inhibition,<sup>27</sup> attesting to the novelty of our discovery. As far as we are aware, with the exception of *G. mangostana*<sup>49</sup> this is the first time these plants have been reported to have antineuraminidase activity.

Despite our success identifying true inhibitors, it is curious that the correlation between predicted free energies and experimentally measured potencies was poor. As Warren et al. demonstrated in their critical assessment of nine docking tools,<sup>66</sup> this is a general problem independent of the docking program used. One of the advantages of the method herein described is that it does not rely on a single docking score. Docking scores were used only to guide

the selection of appropriate plants, each containing *multiple* predicted NA inhibitors, for further experimental examination.

## CONCLUSION

We identified five tropical plants that show inhibitory activity against H5N1 neuraminidase: *G. mangostana*, *E. longifolia*, *T. divaricata*, *B. javanica*, and *M. charantia*. Parts of these plants—leaves, roots, and fruits—were subjected to various extraction methods, chromatographed, and further fractionated for biological testing. Fractions and extracts of the five plants exhibited good to moderate anti-H5N1 neuraminidase activity. *G. mangostana* had the highest inhibition (82.95% at 250  $\mu\text{g}/\text{mL}$ ). Pure compounds were subsequently isolated from the five plants. Rubraxanthone,  $\alpha$ -mangostin, and garcinone C, with  $\text{IC}_{50}$  values ranging from 89.71 to 95.49  $\mu\text{M}$ , were particularly notable.

While we are hopeful that further optimization of these compounds will yield more potent analogs, we acknowledge that currently approved NA-inhibiting therapeutics are much stronger binders. The primary purpose of this study is to present a novel computational method for prioritizing biologically active plants for subsequent pharmacological study. The work described here affords a glimpse into the potential of both virtual screening and the NADI compound library, which contains a growing number of Malaysian natural-plant products. We expect that similar virtual-screening approaches will serve as useful tools to guide the future identification of additional bioactive, medicinal plants.

## ASSOCIATED CONTENT

### Supporting Information

A description of the extraction, fractionation, and isolation of specific compounds is provided. Figures of the percent H5N1 NA inhibition for the five plant fractions (Figure S1), plants' compounds (Figure S2), and *G. mangostana* compounds with and without the presence of Triton-X (Figure S3). Table with the NADI virtual-screen results, ranked according to the predicted free energy of binding (Table S1), and the top hits from the NADI virtual screen, grouped according to the associated source plants (Table S2). This material is available free of charge via the Internet at <http://pubs.acs.org>

## AUTHOR INFORMATION

### Corresponding Author

\*Phone: 604-6533888 ext 2206, 2238. Fax: 604-6570017. E-mail: [habibahw@usm.my](mailto:habibahw@usm.my).

### Notes

The authors declare no competing financial interest.

## ACKNOWLEDGMENTS

This work was supported by a Universiti Sains Malaysia Research University grant (304/PFARMASI/633069); a Malaysian Ministry of Science, Technology and Innovation grant through the Nutraceuticals R&D Initiative (09-05-IFN-MEB 004); the National Institutes of Health through the NIH Director's New Innovator Award Program DP2-OD007237; and the NSF TeraGrid Supercomputer resources grant RAC CHE060073N to R.E.A.

## REFERENCES

(1) Webster, R. G.; Peiris, M.; Chen, H. L.; Guan, Y. H5N1 Outbreaks and Enzootic Influenza. *Emerging Infect. Dis* **2006**, *12*, 3–8.

(2) Itzstein, M. V.; Thomson, R. Anti-Influenza Drugs: The Development of Sialidase Inhibitors. In *Antiviral Strategies, Handbook of Experimental 111 Pharmacology*; Kräusslich, H. G., Bartenschlager, R., Eds.; Springer-Verlag: Berlin, 2009; p 189.

(3) Colman, P. M. Influenza Virus Neuraminidase: Structure, Antibodies, and Inhibitors. *Protein Sci* **1994**, *3*, 1687–1696.

(4) Haskell, T. H.; Peterson, F. E.; Watson, D.; Plessas, N. R.; Culberts, T. Neuraminidase Inhibition and Viral Chemotherapy. *J. Med. Chem* **1970**, *13*, 697–704.

(5) Gong, J. Z.; Xu, W. F.; Zhang, J. Structure and Functions of Influenza Virus Neuraminidase. *Curr. Med. Chem* **2007**, *14*, 113–122.

(6) Gubareva, L. V.; Kaiser, L.; Hayden, F. G. Influenza Virus Neuraminidase Inhibitors. *Lancet* **2000**, *355*, 827–835.

(7) Burmeister, W. P.; Ruigrok, R. W. H.; Cusack, S. The 2.2-Å Resolution Crystal-Structure of Influenza-B Neuraminidase and Its Complex with Sialic-Acid. *EMBO J* **1992**, *11*, 49–56.

(8) von Itzstein, M. The War against Influenza: Discovery and Development of Sialidase Inhibitors. *Nat. Rev. Drug Discovery* **2007**, *6*, 967–974.

(9) De Clercq, E. Antiviral Agents Active against Influenza A Viruses. *Nat. Rev. Drug Discovery* **2006**, *5*, 1015–1025.

(10) Coombes, R. U. Stocks up on Antiviral Drug to Tackle Flu Outbreak. *BMJ* **2005**, *330*, 495–495.

(11) Jennings, L. C.; Monto, A. S.; Chan, P. K. S.; Szucs, T. D.; Nicholson, K. G. Stockpiling Prepandemic Influenza Vaccines: A New Cornerstone of Pandemic Preparedness Plans. *Lancet Infect. Dis* **2008**, *8*, 650–658.

(12) Kamali, A.; Holodniy, M. Influenza Treatment and Prophylaxis with Neuraminidase Inhibitors: A Review. *Infect. Drug Resist* **2013**, *6*, 187–198.

(13) Dawood, F. S.; Jain, S.; Finelli, L.; Shaw, M. W.; Lindstrom, S.; Garten, R. J.; Gubareva, L. V.; Xu, X. Y.; Bridges, C. B.; Uyeki, T. M. Emergence of a Novel Swine-Origin Influenza A (H1N1) Virus in Humans. *N. Engl. J. Med* **2009**, *360*, 2605–2615.

(14) Meijer, A.; Lackenby, A.; Hungnes, O.; Lina, B.; van der Werf, S.; Schweiger, B.; Opp, M.; Paget, J.; van de Kassteele, J.; Hay, A.; Zambon, M.; Sc, E. I. S. Oseltamivir-Resistant Influenza Virus A (H1N1), Europe, 2007–08 Season. *Emerging Infect. Dis* **2009**, *15*, 552–560.

(15) Moscona, A. Global Transmission of Oseltamivir-Resistant Influenza. *N. Engl. J. Med* **2009**, *360*, 953–956.

(16) de Jong, M. D.; Tran, T. T.; Truong, H. K.; Vo, M. H.; Smith, G. J.; Nguyen, V. C.; Bach, V. C.; Phan, T. Q.; Do, Q. H.; Guan, Y.; Peiris, J. S.; Tran, T. H.; Farrar, J. Oseltamivir Resistance During Treatment of Influenza A (H5N1) Infection. *N. Engl. J. Med* **2005**, *353*, 2667–2672.

(17) Blundell, T. L.; Sibanda, B. L.; Montalvo, R. W.; Brewerton, S.; Chelliah, V.; Worth, C. L.; Harmer, N. J.; Davies, O.; Burke, D. Structural Biology and Bioinformatics in Drug Design: Opportunities and Challenges for Target Identification and Lead Discovery. *Philos. Trans. R. Soc., B* **2006**, *361*, 413–423.

(18) Rakers, C.; Schwerdtfeger, S. M.; Mortier, J.; Duwe, S.; Wolff, T.; Wolber, G.; Melzig, M. F. Inhibitory Potency of Flavonoid Derivatives on Influenza Virus Neuraminidase. *Bioorg. Med. Chem. Lett* **2014**, *24*, 4312–4317.

(19) Shan, Y. Y.; Ma, Y.; Wang, M. Y.; Dong, Y. L. Recent Advances in the Structure-Based Design of Neuraminidase Inhibitors as Anti-Influenza Agents. *Curr. Med. Chem* **2012**, *19*, 5885–5894.

(20) Feng, E. G.; Ye, D. J.; Li, J.; Zhang, D. Y.; Wang, J. F.; Zhao, F.; Hilgenfeld, R.; Zheng, M. Y.; Jiang, H. L.; Liu, H. Recent Advances in Neuraminidase Inhibitor Development as Anti-Influenza Drugs. *ChemMedChem* **2012**, *7*, 1527–1536.

(21) Dave, K.; Gandhi, M.; Panchal, H.; Vaidya, M. Revision of Qsar, Docking, and Molecular Modeling Studies of Anti-Influenza Virus A (H1N1) Drugs and Targets: Analysis of Hemagglutinins 3d Structure. *Curr. Comput.-Aided Drug Des* **2011**, *7*, 255–262.

(22) Wang, J. Z.; Ma, C. L.; Wang, J.; Jo, H.; Canturk, B.; Fiorin, G.; Pinto, L. H.; Lamb, R. A.; Klein, M. L.; DeGrado, W. F. Discovery of Novel Dual Inhibitors of the Wild-Type and the Most Prevalent

Drug-Resistant Mutant, S31N, of the M2 Proton Channel from Influenza A Virus. *J. Med. Chem.* **2013**, *56*, 2804–2812.

(23) Gkeka, P.; Eleftheratos, S.; Kolocouris, A.; Cournia, Z. Free Energy Calculations Reveal the Origin of Binding Preference for Aminoadamantane Blockers of Influenza A/M2tm Pore. *J. Chem. Theory Comput.* **2013**, *9*, 1272–1281.

(24) Harvey, A. L. Natural Products in Drug Discovery. *Drug Discovery Today* **2008**, *13*, 894–901.

(25) Newman, D. J.; Cragg, G. M. Natural Product Scaffolds as Leads to Drugs. *Future Med. Chem.* **2009**, *1*, 1415–1427.

(26) Nagai, T.; Moriguchi, R.; Suzuki, Y.; Tomimori, T.; Yamada, H. Mode of Action of the Anti-Influenza Virus Activity of Plant Flavonoid, 5,7,4'-Trihydroxy-8-Methoxyflavone, from the Roots of *Scutellaria Baicalensis*. *Antiviral Res.* **1995**, *26*, 11–25.

(27) Grienke, U.; Schmidtke, M.; von Grafenstein, S.; Kirchmair, J.; Liedl, K. R.; Rollinger, J. M. Influenza Neuraminidase: A Druggable Target for Natural Products. *Nat. Prod. Rep.* **2012**, *29*, 11–36.

(28) Wahab, H. A.; Asarudin, M. R.; Ahmad, S.; Mohamed, N.; Rahim, A. S. A.; Hamid, S. A.; Osman, H.; Shamsudin, S. *Nature Based Drug Discovery (Nadi) & Its Application to Novel Neuraminidase Inhibitors Identification by Virtual Screening, Pharmacophore Modelling and Mapping of Malaysian Medicinal Plants*; ICS-UNIDO: Trieste, Italy, 2009.

(29) Petersen, F. D.; René, A. *Natural Compounds as Drugs*; Springer: London, 2008.

(30) Ogungbe, I. V.; Setzer, W. N. Comparative Molecular Docking of Antitrypanosomal Natural Products into Multiple Trypanosoma Brucei Drug Targets. *Molecules* **2009**, *14*, 1513–1536.

(31) Phosrithong, N.; Ungwitayatorn, J. Molecular Docking Study on Anticancer Activity of Plant-Derived Natural Products. *Med. Chem. Res.* **2010**, *19*, 817–835.

(32) Li, C.; Xu, L.; Wolan, D. W.; Wilson, I. A.; Olson, A. J. Virtual Screening of Human 5-Aminoimidazole-4-Carboxamide Ribonucleotide Transferase against the Nci Diversity Set by Use of Autodock to Identify Novel Nonfolate Inhibitors. *J. Med. Chem.* **2004**, *47*, 6681–6690.

(33) Rollinger, J. M.; Steindl, T. M.; Schuster, D.; Kirchmair, J.; Anrain, K.; Ellmerer, E. P.; Langer, T.; Stuppner, H.; Wutzler, P.; Schmidtke, M. Structure-Based Virtual Screening for the Discovery of Natural Inhibitors for Human Rhinovirus Coat Protein. *J. Med. Chem.* **2008**, *51*, 842–851.

(34) Lipinski, C. A. Lead- and Drug-Like Compounds: The Rule-of-Five Revolution. *Drug Discovery Today: Technol.* **2004**, *1*, 337–341.

(35) Liu, T.; Lin, Y.; Wen, X.; Jorissen, R. N.; Gilson, M. K. Bindingdb: A Web-Accessible Database of Experimentally Determined Protein-Ligand Binding Affinities. *Nucleic Acids Res.* **2007**, *35*, D198–201.

(36) Chen, X.; Lin, Y.; Liu, M.; Gilson, M. K. The Binding Database: Data Management and Interface Design. *Bioinformatics* **2002**, *18*, 130–139.

(37) Greenwood, J. R.; Calkins, D.; Sullivan, A. P.; Shelley, J. C. Towards the Comprehensive, Rapid, and Accurate Prediction of the Favorable Tautomeric States of Drug-Like Molecules in Aqueous Solution. *J. Comput.-Aided Mol. Des.* **2010**, *24*, 591–604.

(38) Shelley, J. C.; Cholleti, A.; Frye, L. L.; Greenwood, J. R.; Timlin, M. R.; Uchimaya, M. Epik: A Software Program for Pk(a) Prediction and Protonation State Generation for Drug-Like Molecules. *J. Comput.-Aided Mol. Des.* **2007**, *21*, 681–691.

(39) Jorgensen, W. L.; Maxwell, D. S.; TiradoRives, J. Development and Testing of the Opls All-Atom Force Field on Conformational Energetics and Properties of Organic Liquids. *J. Am. Chem. Soc.* **1996**, *118*, 11225–11236.

(40) Kaminski, G. A.; Friesner, R. A.; Tirado-Rives, J.; Jorgensen, W. L. Evaluation and Reparametrization of the Opls-Aa Force Field for Proteins Via Comparison with Accurate Quantum Chemical Calculations on Peptides. *J. Phys. Chem. B* **2001**, *105*, 6474–6487.

(41) Sanner, M. F. A Component-Based Software Environment for Visualizing Large Macromolecular Assemblies. *Structure* **2005**, *13*, 447–462.

(42) Russell, R. J.; Haire, L. F.; Stevens, D. J.; Collins, P. J.; Lin, Y. P.; Blackburn, G. M.; Hay, A. J.; Gamblin, S. J.; Skehel, J. J. The Structure of

H5N1 Avian Influenza Neuraminidase Suggests New Opportunities for Drug Design. *Nature* **2006**, *443*, 45–49.

(43) Morris, G. M.; Goodsell, D. S.; Halliday, R. S.; Huey, R.; Hart, W. E.; Belew, R. K.; Olson, A. J. Automated Docking Using a Lamarckian Genetic Algorithm and an Empirical Binding Free Energy Function. *J. Comput. Chem.* **1998**, *19*, 1639–1662.

(44) Weiner, S. J.; Kollman, P. A.; Case, D. A.; Singh, U. C.; Ghio, C.; Alagona, G.; Profeta, S.; Weiner, P. A New Force Field for Molecular Simulation of Nucleic Acids and Proteins. *J. Am. Chem. Soc.* **1984**, *106*, 765–784.

(45) Gasteiger, J.; Marsili, M. Iterative Partial Equalization of Orbital Electronegativity—a Rapid Access to Atomic Charges. *Tetrahedron* **1980**, *36*, 3219–3228.

(46) Morris, G. M.; Goodsell, D. S.; Huey, R.; Hart, W. E.; Halliday, S.; Belew, R.; Olson, A. J. *Autodock: Automated Docking of Flexible Ligands to Receptors*, version 3.0.5; Scripps Research Institute: San Diego, California, 2001.

(47) Potier, M.; Mameli, L.; Belisle, M.; Dallaire, L.; Melancon, S. B. Fluorometric Assay of Neuraminidase with a Sodium (4-Methylumbelliferyl- $\alpha$ -D-N-Acetylneuraminat) Substrate. *Anal. Biochem.* **1979**, *94*, 287–296.

(48) Feng, B. Y.; Shoichet, B. K. A Detergent-Based Assay for the Detection of Promiscuous Inhibitors. *Nat. Protoc.* **2006**, *1*, 550–553.

(49) Ryu, H. W.; Curtis-Long, M. J.; Jung, S.; Jin, Y. M.; Cho, J. K.; Ryu, Y. B.; Lee, W. S.; Park, K. H. Xanthenes with Neuraminidase Inhibitory Activity from the Seedcases of *Garcinia Mangostana*. *Bioorg. Med. Chem.* **2010**, *18*, 6258–6264.

(50) Obolskiy, D.; Pischel, I.; Siriwatanametanon, N.; Heinrich, M.; *Garcinia Mangostana*, L. A Phytochemical and Pharmacological Review. *Phytother. Res.* **2009**, *23*, 1047–1065.

(51) Pedraza-Chaverri, J.; Cardenas-Rodriguez, N.; Orozco-Ibarra, M.; Perez-Rojas, J. M. Medicinal Properties of Mangosteen (*Garcinia Mangostana*). *Food Chem. Toxicol.* **2008**, *46*, 3227–3239.

(52) Lian, G. E. C.; Rahmani, M. B. Available from <http://km.upm.edu.my/kmportalweb/infox/assetDetailAction.action?execute=view&assetId=000001421&actionFlg=alllist>.

(53) Ryu, Y. B.; Curtis-Long, M. J.; Lee, J. W.; Kim, J. H.; Kim, J. Y.; Kang, K. Y.; Lee, W. S.; Park, K. H. Characteristic of Neuraminidase Inhibitory Xanthenes from *Cudrania Tricuspidata*. *Bioorg. Med. Chem.* **2009**, *17*, 2744–2750.

(54) Feng, B. Y.; Simeonov, A.; Jadhav, A.; Babaoglu, K.; Inglese, J.; Shoichet, B. K.; Austin, C. P. A High-Throughput Screen for Aggregation-Based Inhibition in a Large Compound Library. *J. Med. Chem.* **2007**, *50*, 2385–2390.

(55) Friesner, R. A.; Banks, J. L.; Murphy, R. B.; Halgren, T. A.; Klicic, J. J.; Mainz, D. T.; Repasky, M. P.; Knoll, E. H.; Shelley, M.; Perry, J. K.; Shaw, D. E.; Francis, P.; Shenkin, P. S. Glide: A New Approach for Rapid, Accurate Docking and Scoring. 1. Method and Assessment of Docking Accuracy. *J. Med. Chem.* **2004**, *47*, 1739–1749.

(56) Halgren, T. A.; Murphy, R. B.; Friesner, R. A.; Beard, H. S.; Frye, L. L.; Pollard, W. T.; Banks, J. L. Glide: A New Approach for Rapid, Accurate Docking and Scoring. 2. Enrichment Factors in Database Screening. *J. Med. Chem.* **2004**, *47*, 1750–1759.

(57) Durrant, J. D.; McCammon, J. A. Binana: A Novel Algorithm for Ligand-Binding Characterization. *J. Mol. Graphics Modell.* **2011**, *29*, 888–893.

(58) Stierand, K.; Maass, P. C.; Rarey, M. Molecular Complexes at a Glance: Automated Generation of Two-Dimensional Complex Diagrams. *Bioinformatics* **2006**, *22*, 1710–1716.

(59) Stierand, K.; Rarey, M. Drawing the Pdb: Protein-Ligand Complexes in Two Dimensions. *ACS Med. Chem. Lett.* **2010**, *1*, 540–545.

(60) Humphrey, W.; Dalke, A.; Schulten, K. Vmd: Visual Molecular Dynamics. *J. Mol. Graphics* **1996**, *14*, 33–38.

(61) Amaro, R. E.; Swift, R. V.; Votapka, L.; Li, W. W.; Walker, R. C.; Bush, R. M. Mechanism of 150-Cavity Formation in Influenza Neuraminidase. *Nat. Commun.* **2011**, *2*, 388.

(62) Wu, Y.; Qin, G. R.; Gao, F.; Liu, Y.; Vavricka, C. J.; Qi, J. X.; Jiang, H. L.; Yu, K. Q.; Gao, G. F. Induced Opening of Influenza Virus



Neuraminidase N2 150-Loop Suggests an Important Role in Inhibitor Binding. *Sci. Rep.* **2013**, *3*, 1551.

(63) Sharma, A.; Tendulkar, A. V.; Wangikar, P. P. Drug Discovery against H1N1 Virus (Influenza A Virus) Via Computational Virtual Screening Approach. *Med. Chem. Res.* **2011**, *20*, 1445–1449.

(64) Saha, R. K.; Takahashi, T.; Suzuki, T. Glucosyl Hesperidin Prevents Influenza A Virus Replication in Vitro by Inhibition of Viral Sialidase. *Biol. Pharm. Bull.* **2009**, *32*, 1188–1192.

(65) Wang, X. Y.; Jia, W.; Zhao, A. H.; Wang, X. R. Anti-Influenza Agents from Plants and Traditional Chinese Medicine. *Phytother. Res.* **2006**, *20*, 335–341.

(66) Warren, G. L.; Andrews, C. W.; Capelli, A. M.; Clarke, B.; LaLonde, J.; Lambert, M. H.; Lindvall, M.; Nevins, N.; Semus, S. F.; Senger, S.; Tedesco, G.; Wall, I. D.; Woolven, J. M.; Peishoff, C. E.; Head, M. S. A Critical Assessment of Docking Programs and Scoring Functions. *J. Med. Chem.* **2006**, *49*, 5912–5931.